Oxidative Addition of Halogens to $[Pt(S_2N_2H)(PR_3)_2]BF_4$. X-Ray Crystal Structures of $[Pt(S_2N_2H)X(PMe_2Ph)]$ (X = Br or I) and the Monoclinic and Triclinic Polymorphs of $[Pt(S_2N_2H)Br_2(PMe_2Ph)_2]BF_4$†

Ray Jones, Paul F. Kelly, David J. Williams, and J. Derek Woollins*
Department of Chemistry, Imperial College of Science and Technology, South Kensington, London SW7 2AY

$[Pt(S_2N_2H)(PMe_2Ph)_2]BF_4$ (**1a**) reacts with bromine to give the Pt^{IV} *trans*-dibromo compound $[Pt(S_2N_2H)Br_2(PMe_2Ph)_2]BF_4$ (**2**). This rapidly isomerises to the *cis* isomer (α and β forms) which readily undergoes reductive elimination to give $[Pt(S_2N_2H)Br(PMe_2Ph)]$ (**3**). $[Pt(S_2N_2H)I(PMe_2Ph)]$ (**4**) was obtained by the reaction of (**1a**) with iodine. Similarly, treatment of $[Pt(S_2N_2H)(PR_3)_2]BF_4$ (PR_3 = PMe_3 or PPr^n_3) with bromine leads to $[Pt(S_2N_2H)Br(PR_3)]$. The α and β forms of (**2**) together with (**3**) and (**4**) have been characterised by *X*-ray crystallography.

Previously we have reported on the preparation of compounds of the type $[M(S_2N_2H)(PR_3)_2]X$ (M = Pt or Pd; X = BF_4^-, PF_6^-, or Cl^-) in which the $S_2N_2H^-$ ligand forms part of a five-membered metallacycle, protonated on the nitrogen bound to the metal.[1,2] In the solid state the compounds of smaller phosphines, PMe_3 or PMe_2Ph, are of special interest since they exhibit infinite stacking arrangements which are unique for Pt or Pd phosphine complexes.[3,4]

Here we report on the reactions of $[Pt(S_2N_2H)(PMe_2Ph)_2]BF_4$ (**1a**) and $[Pt(S_2N_2H)(PMe_3)_2]BF_4$ (**1b**) with halogens (Br_2 or I_2) which result in the formation of Pt^{IV} dihalogeno species. In the case of the reaction of (**1a**) with bromine, the initial product is the *trans*-dibromo isomer of $[Pt(S_2N_2H)Br_2(PMe_2Ph)_2]BF_4$ which rapidly undergoes isomerisation to the *cis* isomer, as revealed by ^{31}P n.m.r.

The Pt^{IV} compounds readily undergo reductive elimination to give Pt^{II} compounds of the type $[Pt(S_2N_2H)X(PR_3)]$ which also exhibit interesting packing features.

Experimental

All procedures were carried out under an inert atmosphere (N_2 or Ar). Prior to use Et_2O and hexane were distilled from sodium; CH_2Cl_2 and MeCN were distilled from calcium hydride. Bromine was used as received. ^{31}P-$\{^1H\}$ N.m.r. spectra were measured using a JEOL FX90Q spectrometer operating at 36.21 MHz and are referred to external 85% H_3PO_4. Elemental analyses were performed by the microanalytical department of Imperial College.

The compounds $[Pt(S_2N_2H)(PR_3)_2]BF_4$ [PR_3 = PMe_2Ph (**1a**) or PMe_3 (**1b**)] were prepared as described previously.[2] Analytical data are given in Table 1 and spectroscopic data in Table 2.

Preparation of trans-$[Pt(S_2N_2H)Br_2(PMe_2Ph)_2]BF_4$.—A solution of (**1a**) (0.2 g, 3.1×10^{-4} mol) in CH_2Cl_2 (10 cm^3) was treated with a solution of bromine in CH_2Cl_2 (1.6 cm^3, 3.1×10^{-4} mol) added over a period of *ca.* 30 s. The resulting dark red solution was reduced to 2 cm^3 *in vacuo* and the crude product precipitated as a dark claret solid by addition of Et_2O (50 cm^3). After washing with $CHCl_3$ (2×5 cm^3) at −20 °C the solid analysed correctly for the desired product. Yield: 0.21 g (84%).

† Bromo[di(azathien)-1-yl-S^1N^4](dimethylphenylphosphine)-platinum(II), [di(azathien)-1-yl-S^1N^4](dimethylphenylphosphine)iodo-platinum(II), and *cis*-dibromo[di(azathien)-1-yl-S^1N^4]bis(dimethyl-phenylphosphine)platinum(IV) tetrafluoroborate.

Supplementary data available: see Instructions for Authors, *J. Chem. Soc., Dalton Trans.*, 1988, Issue 1, pp. xvii—xx.

Table 1. Analytical data (%)*

Compound		C	H	N
(**2**) $[Pt(S_2N_2H)Br_2(PMe_2Ph)_2]BF_4$	*trans*	23.8	2.8	3.3
		(23.7)	(2.9)	(3.5)
	α *cis*	23.8	2.8	3.4
		(23.7)	(2.9)	(3.5)
	β *cis*	23.5	2.8	3.4
		(23.7)	(2.9)	(3.5)
(**3**) $[Pt(S_2N_2H)Br(PMe_2Ph)]$		19.0	2.2	5.4
		(19.0)	(2.4)	(5.5)
(**4**) $[Pt(S_2N_2H)I(PMe_2Ph)]$		17.3	2.1	5.0
		(17.4)	(2.2)	(5.1)
(**6**) $[Pt(S_2N_2H)Br(PMe_3)]$		8.8	2.0	6.1
		(8.1)	(2.3)	(6.3)

* Calculated values are given in parentheses.

Preparation of Crystalline cis-$[Pt(S_2N_2H)Br_2(PMe_2Ph)_2]BF_4$.—The above reaction was repeated and the crude product extracted into a hot CH_2Cl_2–$CHCl_3$ mixture (1:1, *ca.* 3 cm^3). The resulting solution was cooled to −20 °C overnight during which time large, well formed orange-red crystals of the α product were deposited, and were retrieved by decanting off the mother-liquor and washed with cold $CHCl_3$. Yield: 0.14 g (56%). A mixture of β and α forms was obtained by dissolving the *trans* complex from the above reaction in CH_2Cl_2 (3 cm^3) and layering n-hexane on top of this solution (at room temperature). The proportion of β and α material obtained was variable.

Preparation of $[Pt(S_2N_2H)Br(PMe_2Ph)]$.—A solution of (**1a**) (0.16 g, 2.5×10^{-4} mol) in CH_2Cl_2 (10 cm^3) was treated with bromine solution in CH_2Cl_2 (1.3 cm^3, 2.5×10^{-4} mol), and after stirring for 5 min, a dark solid was precipitated with Et_2O (50 cm^3). This was redissolved in CH_3CN–CH_2Cl_2 (1:2, 20 cm^3) and the resulting solution allowed to stand for two weeks. After this time the solvent was evaporated off *in vacuo* and the product taken into CH_2Cl_2 (2 cm^3) and placed on a preparative t.l.c. plate. Elution with CH_2Cl_2 revealed a bright yellow-orange band (R_f *ca.* 0.5) which was removed and the product washed off with MeOH. After removal of the MeOH *in vacuo* the residue was taken into CH_2Cl_2 (1 cm^3), hexane (20 cm^3) added, and the product obtained as well formed microcrystals by evaporation of the CH_2Cl_2 *in vacuo*. Yield: *ca.* 21 mg (17%).

Preparation of $[Pt(S_2N_2H)I(PMe_2Ph)]$.—A solution of (**1a**) (0.1 g, 1.5×10^{-4} mol) in CH_2Cl_2 (10 cm^3) was treated with a

Table 2. I.r. and ^{31}P n.m.r. data[a]

Compound			δ_A (^1J/Hz)	δ_B (^1J/Hz)	^2J/Hz	ν(NH)	ν(SN)	δ(SN)
(2) $[Pt(S_2N_2H)Br_2(PMe_2Ph)_2]BF_4$	*trans*[b]		−19.1 (1 615)	−28.7 (2 117)	10	3 190	*c*	310
	α *cis*	} *d*	2.0 (2 134)	−19.9 (2 122)	10	3 170	*c*	324
	β *cis*					3 130		325
(3) $[Pt(S_2N_2H)Br(PMe_2Ph)]$[e]			−23.5 (3 367)			3 190	1 040	345
(4) $[Pt(S_2N_2H)I(PMe_2Ph)]$[e]			−25.6 (3 416)			3 220	1 035	340
(5) $[Pt(S_2N_2H)Br_2(PMe_3)_2]BF_4$[b]			−14.5 (1 641)	−21.3 (2 064)	14		*f*	
(6) $[Pt(S_2N_2H)Br(PMe_3)]$[b]			−33.0 (3 355)			3 275	1 030, 695	335
$[Pt(S_2N_2H)Br(PPr^n_3)]$[e]			−3.7 (3 294)				*f*	

[a] ^{31}P N.m.r. data are referred to external 85% H_3PO_4. [b] $CDCl_3$–CH_3CN Solution. [c] Obscured by BF_4^-. [d] CD_3CN Solution. [e] $CDCl_3$ Solution. [f] Compound not isolated.

solution of I_2 (40 mg, 1.6×10^{-4} mol) in warm CH_2Cl_2 (10 cm^3) to give a dark purple solution which was allowed to stand for 4 d. After this time silica gel (0.2 g) was added to the solution, in air, and the mixture stirred for *ca.* 30 min. The silica was washed with CH_2Cl_2 (5×15 cm^3) until the washings were colourless and the resulting solution concentrated to *ca.* 2 cm^3 *in vacuo*. The solution was then placed on a preparative t.l.c. plate and eluted with CH_2Cl_2. The orange band (R_f 0.6) was removed, extracted into MeOH, and the product isolated in the same manner as the bromo analogue, as orange-brown microcrystals. Yield: 15 mg (18%).

Preparation of $[Pt(S_2N_2H)Br(PMe_3)]$.—A solution of (**1b**) (0.08 g, 1.5×10^{-4} mol) in CH_2Cl_2 (10 cm^3) was treated with bromine solution in CH_2Cl_2 (0.8 cm^3, 1.6×10^{-4} mol) and the resulting dark red solution stirred for 5 min. It was then reduced to 2 cm^3 *in vacuo* and a dark solid precipitated on the addition of Et_2O–hexane (3:1, 70 cm^3). After drying *in vacuo* the solid was redissolved in CH_2Cl_2 (20 cm^3) and crystallisation attempted by slow diffusion of hexane (50 cm^3). After one week no crystals were apparent, only an amorphous red solid and a yellow-orange solution. The solution was filtered and evaporated to dryness *in vacuo*.

The residue was extracted into CH_2Cl_2 (1 cm^3) and hexane (20 cm^3) added to precipitate a brown solid. This was redissolved by heating the mixture and crystallised by cooling overnight. Yield: *ca.* 5 mg (8%).

Preparation of $[Pt(S_2N_2H)Br(PPr^n_3)]$.—A solution of $[Pt(S_2N_2H)(PPr^n_3)_2]BF_4$ (0.27 g, 3.9×10^{-4} mol) in CH_2Cl_2 (10 cm^3) was treated with bromine solution in CH_2Cl_2 (2.0 cm^3, 3.9×10^{-4} mol) to give a dark red product. The solvent was removed *in vacuo* and the resulting oily solid thoroughly dried to remove all the bromine. The resulting red solid was redissolved in CH_2Cl_2 (30 cm^3) and allowed to stand. The solution was monitored by t.l.c.; after 1 d elution with CH_2Cl_2 revealed only a red non-moving band and a purple band at R_f 0.3. After 2 d the desired product was visible as an orange band, R_f 0.5, which became stronger with time. After 5 d the solvent was removed *in vacuo* and the oily product extracted into Et_2O (6×20 cm^3) and filtered; the Et_2O was then removed and the residue taken into CH_2Cl_2 (2 cm^3) and run on a preparative t.l.c. plate in the same manner as the previous examples. The ^{31}P n.m.r. of the product is consistent with the formulation although the product could only be isolated as an oil due to its high solubility. Yield: 30 mg (15%).

X-*Ray Structure Determination.*—*Crystal data.* $[Pt(S_2N_2H)Br_2(PMe_2Ph)_2]BF_4$ (**2α**). $C_{16}H_{23}BBr_2F_4N_2P_2PtS_2$, M = 811.15, monoclinic, a = 10.572(6), b = 8.507(2), c = 18.153(4) Å, β = 110.00(2)°, U = 2 550(1) Å^3, space group $P2_1/n$, Z = 4, D_c = 2.12 g cm^{-3}, μ(Cu-K_α) = 172 cm^{-1}, λ = 1.541 78 Å, F(000) = 1 536. Red air-stable plate, crystal dimensions 0.15 × 0.15 × 0.03 mm.

$[Pt(S_2N_2H)Br_2(PMe_2Ph)_2]BF_4$ (**2β**). $C_{16}H_{23}BBr_2F_4N_2P_2PtS_2$, M = 811.15, triclinic, a = 10.667(3), b = 10.785(3), c = 11.250(2) Å, α = 83.24(2), β = 89.37(2), γ = 77.39(2)°, U = 1 254.1(5) Å^3, space group $P\bar{1}$, Z = 2, D_c = 2.16 g cm^{-3}, μ(Cu-K_α) = 175 cm^{-1}, λ = 1.541 78 Å, F(000) = 768. Red air-stable prism, crystal dimensions 0.1 × 0.3 × 0.3 mm.

$[Pt(S_2N_2H)Br(PMe_2Ph)]$ (**3**). $C_8H_{12}BrN_2PPtS_2$, M = 506.26, orthorhombic, a = 6.303(3), b = 13.857(5), c = 16.166(8) Å, U = 1 412(1) Å^3, space group $P2_12_12_1$, Z = 4, D_c = 2.39 g cm^{-3}, μ(Cu-K_α) = 258 cm^{-1}, λ = 1.541 78 Å, F(000) = 936. Thick orange rod, crystal dimensions 0.1 × 0.15 × 0.4 mm.

$[Pt(S_2N_2H)I(PMe_2Ph)]$ (**4**). $C_8H_{12}IN_2PPtS_2$, M = 553.28, orthorhombic, a = 6.616(3), b = 13.887(6), c = 16.195(9) Å, U = 1 488(1) Å^3, space group $P2_12_12_1$, Z = 4, D_c = 2.48 g cm^{-3}, μ(Cu-K_α) = 378 cm^{-1}, λ = 1.541 78 Å, F(000) = 1 008. Orange needle, crystal dimensions 0.1 × 0.05 × 0.4 mm.

Data collection and processing. Nicolet *R3m* diffractometer, ω-scan method [2θ ≤ 116° for (**2β**), (**3**), and (**4**); 2θ ≤ 100° for (**2a**)], graphite-monochromated Cu-K_α radiation. 2 623, 3 380, 1 130, and 1 186 independent measured reflections of which 2 287, 3 322, 1 123, and 1 167 were respectively considered observed [$|F_o| > 3\sigma(|F_o|)$] for (**2α**), (**2β**), (**3**), and (**4**); all were corrected for Lorentz and polarisation factors; Gaussian absorption correction (face indexed crystals) for all data sets.

Structure analysis and refinement. All four structures were solved by the heavy-atom method and the non-hydrogen atoms refined anisotropically, with the exception of four 25% occupancy fluorine sites located from a ΔF map as an alternative orientation of the BF_4 group in (**2β**) which were refined isotropically. In (**2α**) and (**2β**) all orientations of the BF_4 groups were refined as rigid bodies. In all cases the proton attached to the nitrogen atom was located from a ΔF map and idealised. All methyl groups were idealised and refined as rigid bodies. All other hydrogen atoms in all the structures were idealised (C–H = 0.96 Å), assigned isotropic thermal parameters [U(H) = 1.2U_{eq}(C)], and allowed to ride on their parent carbons. Refinement was by the block-cascade full-matrix least-squares method to give for (**2α**) R = 0.044, R' = 0.042 [$w^{-1} = \sigma^2(F) + 0.000\,31F^2$]; for (**2β**) R = 0.037, R' = 0.041 [$w^{-1} = \sigma^2(F) + 0.000\,39F^2$]; for (**3**) R = 0.036, R' = 0.037 [$w^{-1} = \sigma^2(F) + 0.001\,17F^2$]; and for (**4**) R = 0.050, R' = 0.048 [$w^{-1} = \sigma^2(F) + 0.0228F^2$] ($R = \Sigma|F_o - F_c|/\Sigma|F_o|$). The correct chiralities of (**3**) and (**4**) were determined by the refinement of a free variable, η, which multiplies all f'' values. This variable converged to values of −1.22(9) and −1.02(6) for (**3**) and (**4**) respectively and both co-ordinate sets were subsequently inverted. The maximum residual electron densities in the final ΔF maps were 0.94, 1.42, 1.11, and 3.58 e Å^{-3} for (**2α**), (**2β**), (**3**), and (**4**) respectively. The mean and maximum

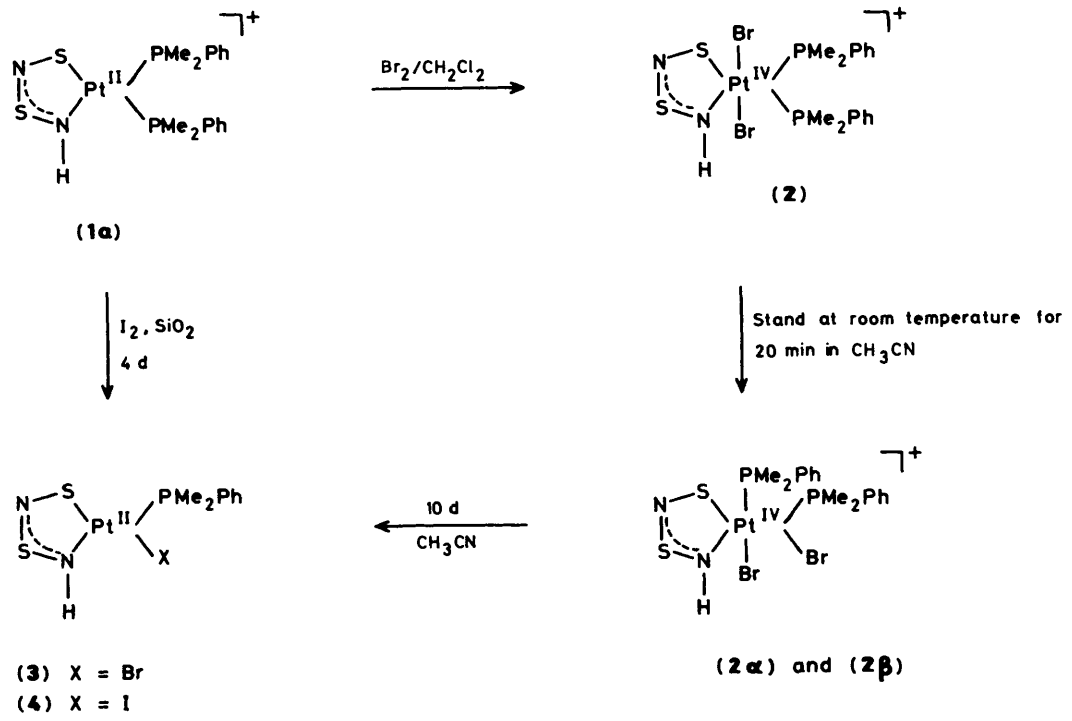

Scheme.

Table 3. Atom co-ordinates (× 10^4) for (2α)

Atom	*x*	*y*	*z*
Pt	−1 094(1)	550(1)	1 578(1)
Br(1)	−346(1)	−1 313(2)	1 012(1)
Br(2)	−1 950(1)	−1 696(2)	1 805(1)
S(1)	−2 814(2)	1 660(5)	446(2)
S(2)	−1 885(2)	2 227(4)	2 031(2)
P(1)	−449(2)	2 748(3)	1 278(2)
P(2)	−139(2)	69(4)	2 802(2)
N(1)	−2 038(6)	716(12)	487(5)
N(2)	−2 709(6)	2 405(14)	1 249(6)
C(1)	−1 103(7)	3 670(14)	384(7)
C(2)	−1 524(8)	5 001(15)	399(8)
C(3)	−2 000(8)	5 674(15)	−311(8)
C(4)	−2 030(8)	5 018(16)	−1 014(8)
C(5)	−1 625(8)	3 675(16)	−1 024(8)
C(6)	−1 169(8)	2 969(15)	−333(7)
C(7)	488(8)	2 368(18)	1 109(8)
C(8)	−222(9)	4 290(16)	1 999(8)
C(9)	−376(7)	1 046(13)	3 560(6)
C(10)	−999(9)	560(17)	3 786(7)
C(11)	−1 217(9)	1 295(18)	4 368(8)
C(12)	−779(11)	2 571(21)	4 734(8)
C(13)	−131(13)	3 044(23)	4 522(11)
C(14)	62(9)	2 310(17)	3 939(8)
C(15)	−65(10)	−1 980(14)	3 080(8)
C(16)	899(7)	554(17)	2 902(9)
F(1)	−2 251(4)	−439(9)	−1 095(4)
F(2)	−3 256(5)	−1 725(10)	−1 931(6)
F(3)	−3 190(6)	831(11)	−2 012(7)
F(4)	−3 471(5)	−238(16)	−1 040(6)
B	−3 042(4)	−393(7)	−1 519(4)

shift/error ratios in the final refinement cycles were for (**2a**) 0.005 and 0.085, for (2β) 0.007 and 0.091, for (**3**) 0.006 and 0.040, and for (**4**) 0.003 and 0.044. Computations were carried out on an Eclipse S140 computer using the SHELXTL [5] program system and published [6] scattering factors. Atomic co-ordinates for (2α), (2β), (**3**), and (**4**) are given in Tables 2—5 respectively. Selected bond lengths and angles are shown in Tables 7—10.

Additional material available from the Cambridge Crystallographic Data Centre comprises thermal parameters, H-atom co-ordinates, and remaining bond lengths and angles.

Results and Discussion

Treatment of $[Pt(S_2N_2H)(PMe_2Ph)_2]BF_4$ (**1a**) with a dilute solution of Br_2 in CH_2Cl_2 gives a dark red solution from which a claret solid can be precipitated with diethyl ether. This solid, after washing with a small volume of cold $CHCl_3$, analyses as the dibromo compound $[Pt(S_2N_2H)Br_2(PMe_2Ph)_2]BF_4$ (**2**) (Scheme).

The ^{31}P n.m.r. of freshly prepared solutions of (**2**) in acetonitrile consist of an asymmetric AX pattern [Figure 1(*a*)], with a small $^2J(^{31}P–^{31}P)$ coupling constant (10 Hz), indicative of the presence of Pt^{IV}. However, this pattern gradually changes to an AB system upon standing; Figure 1(*a*) shows this change with the total time elapsed between spectra (*i*) and (*vi*) being *ca.* 20 min. If a CH_2Cl_2–$CHCl_3$ solution of (*vi*) in Figure 1 is cooled overnight large orange crystals of (2α) are obtained, the ^{31}P n.m.r. spectrum of which is shown in Figure 1(*b*). *X*-Ray crystallography reveals (see later) the bromines in (2α) to be *cis* to each other (Figure 2). The initial product is the *trans* isomer, a conclusion supported by the fact that the ^{31}P n.m.r. of (**1a**) is also very asymmetric and would be likely to retain a roughly equal ratio of ^1J coupling constants upon conversion to the *trans* dibromo species.

To date we have been unable to stabilise the *trans* dibromo species long enough to allow it to be crystallised and so an *X*-ray crystallographic confirmation of the structure has not been possible.

The *cis* isomer of (**2**) can be crystallised in two forms. The α form obtained by the aforementioned cooling method shows hydrogen bonding from the N–H to the BF_4. However, slow hexane diffusion into a CH_2Cl_2 solution of (**2**) yields thinner crystals of the α form together with dark prisms of the β form (Figure 3).

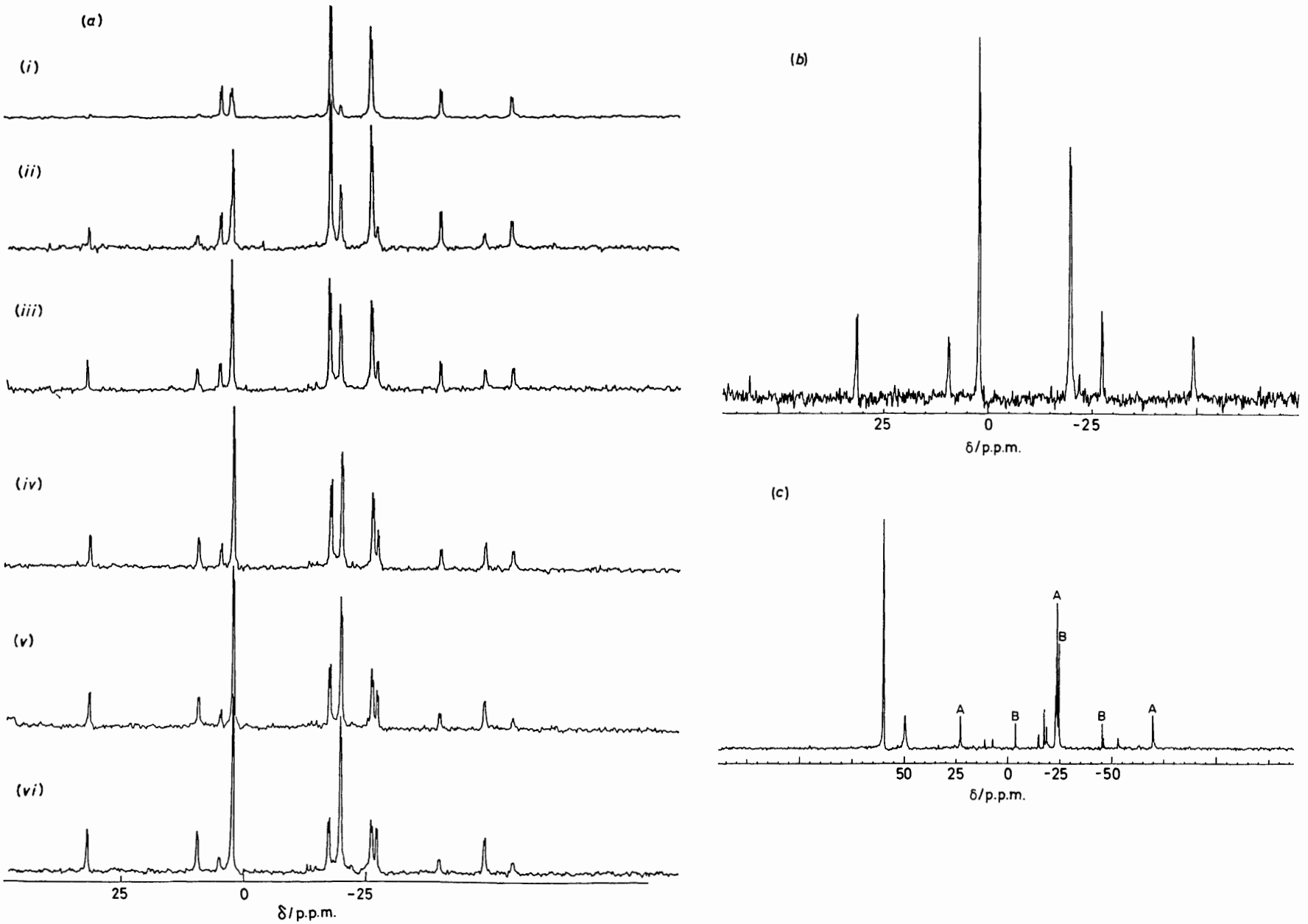

Figure 1. (*a*) ^{31}P N.m.r. spectra of a CD_3CN–CH_3CN solution of $[Pt(S_2N_2H)Br_2(PMe_2Ph)_2]BF_4$ (**2**) taken at time intervals. Spectra (*i*)—(*vi*) were collected over a 20 min period. (*b*) ^{31}P N.m.r. spectrum of a solution of (**2**α) or (**2**β). (*c*) ^{31}P N.m.r. spectrum of solution (*vi*) from (*a*) taken 10 d later (*N.B.* different scales in *x* axis); A indicates peaks due to compound (**3**), B is an unidentified Pt^{IV} compound

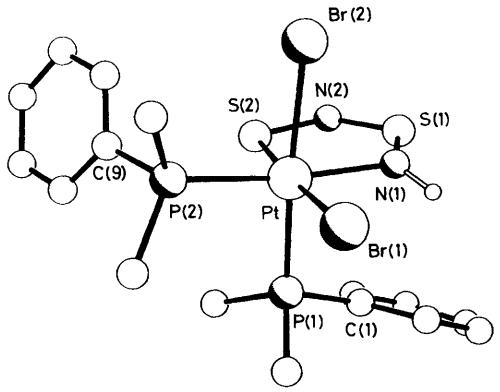

Figure 2. *X*-Ray crystal structure of $[Pt(S_2N_2H)Br_2(PMe_2Ph)_2]BF_4$ (**2α**)

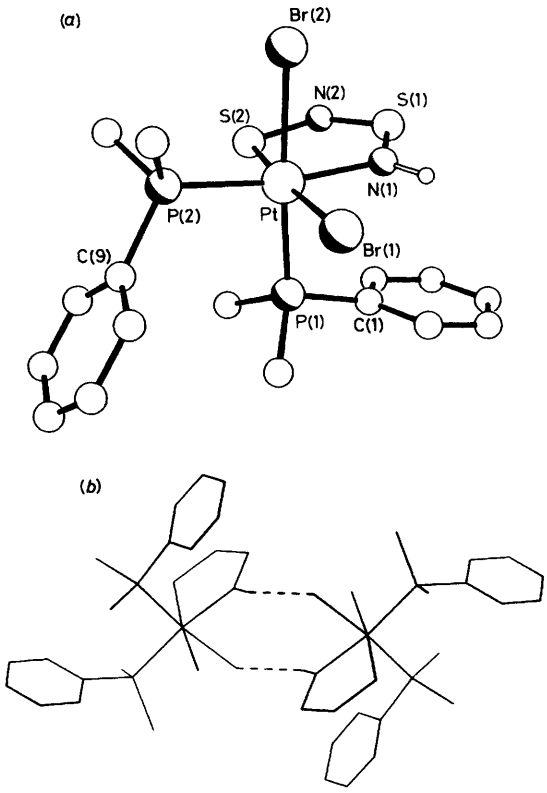

Figure 3. (*a*) *X*-Ray crystal structure of $[Pt(S_2N_2H)Br_2(PMe_2Ph)_2]BF_4$ (**2β**). (*b*) Line drawing of (**2β**) showing hydrogen-bonded dimers

I.r. spectroscopy can distinguish the two forms by their N–H stretches: 3 170 cm^{-1} for (**2α**) compared to 3 130 cm^{-1} for (**2β**). I.r. can also distinguish between the two stereoisomers of (**2**) since the *trans* compound has ν(N–H) at 3 190 cm^{-1} and also shows a single band at 750 cm^{-1} compared to both forms of the *cis* compound which have a doublet in this region (745 and 755 cm^{-1}).

If a solution of (**2**) is allowed to stand, under nitrogen, for a few days the ^{31}P n.m.r. changes quite dramatically. Figure 1(*c*) shows the spectrum of the solution after standing for 10 d. The most obvious features are singlet at δ 60 p.p.m. (typical of a P^V species) together with new platinum complexes at δ −23.5 and −24.5 p.p.m. whose $^1J(^{195}Pt–^{31}P)$ coupling constants (3 367 and 1 776 Hz) are consistent with the presence of Pt^{II} and Pt^{IV} respectively. The new Pt^{II} compound was isolated by preparative t.l.c. (bright yellow-orange band R_f *ca.* 0.5) and *X*-ray analysis of crystals, grown by hexane diffusion into a very concentrated $CHCl_3$ solution, shows the compound to be $[Pt(S_2N_2H)Br(PMe_2Ph)]$ (**3**) (Figure 4). To the best of our knowledge this type of reductive elimination has not been previously reported for platinum complexes.

To date we have been unable to identify the phosphine compound at δ 60 p.p.m. or the Pt^{IV} species. Like (**3**) the latter is very soluble and will even dissolve in warm diethyl ether. It is not clear whether this species is an intermediate in the production of (**3**) or is a separate product and for this reason we cannot be sure of the mechanism of the reaction.

The reductive elimination from (**2**) to (**3**) can also be achieved simply by stirring a solution of (**2**) with silica for a few hours followed by preparative t.l.c. purification. Again we have not been able to ascertain the phosphine–bromine containing side products of the reaction.

The iodo analogue of (**3**) can be prepared in a similar fashion. If (**1a**) is treated with iodine and the resulting solution allowed to stand for a week, and then treated with silica, complex $[Pt(S_2N_2H)I(PMe_2Ph)]$ (**4**) can be isolated by preparative t.l.c. in the same manner as (**3**). *X*-Ray crystallography reveals (Figure 5) an analogous structure to that of (**3**).

The ^{31}P n.m.r. of (**4**) consists of a singlet (δ −25.6 p.p.m.) with a $^1J(^{195}Pt–^{31}P)$ coupling constant of 3 416 Hz. The fact that this coupling is larger than in (**3**) is consistent with the lower electronegativity of iodine which means less electron density is withdrawn from the Pt–phosphine bond. The reaction of (**1**) with iodine is much slower than with bromine but we have not been able to observe intermediates of the type (**2**).

$[Pt(S_2N_2H)(PMe_3)_2]BF_4$ (**1b**) Reacts with bromine, again giving a dark red solution. The ^{31}P n.m.r. spectrum of this product shows an asymmetric AX pattern, consistent with that of the *trans*-dibromo isomer of $[Pt(S_2N_2H)Br_2(PMe_3)_2]$-$BF_4$ (**5**). However, unlike the PMe_2Ph analogue this does not seem to undergo isomerisation, nor can it be crystallised and thus the structure has not been confirmed. Like (**2**) it undergoes reductive elimination upon standing to give $[Pt(S_2N_2H)Br(PMe_3)]$ (**6**). Similarly, treatment of $[Pt(S_2N_2H)(PPr^n_3)_2]BF_4$ with bromine gives a dark solution which, upon standing for a number of days, gives $[Pt(S_2N_2H)Br(PPr^n_3)]$ (**7**). This can be characterised by t.l.c. (bright orange-yellow band, R_F 0.5) and by ^{31}P n.m.r., although the high solubility of the product means that only oils have been isolated. These results suggest that reactions involving trialkylphosphine compounds proceed as for trimethylphosphine, giving eventual products of the type $[Pt(S_2N_2H)Br(PR_3)]$. However, similar reactions involving compounds of PPh_2Me and PPh_3 do not proceed in this manner. Reaction of $[Pt(S_2N_2H)(PPh_3)_2]BF_4$ with bromine is much slower than in the other cases and does not give the expected Pt^{IV} dibromo compound. From ^{31}P n.m.r. the major product is *cis*-$[PtBr_2(PPh_3)_2]$ (δ 1.46 p.p.m., ^1J 3 628 Hz) identical to an authentic sample prepared from $[PtBr_2(cod)]$ (cod = cyclo-octa-1,5-diene). It thus appears that there is a subtle balance between displacement of the $S_2N_2H^-$ ligand or oxidation of the platinum from Pt^{II} to Pt^{IV} in these systems. Phosphines containing more aryl groups favour the displacement reaction, as a consequence of their higher *trans* labilising effect and their poorer ability to stabilise Pt^{IV} compared to more basic trialkylphosphines.

The crystal structures of (**2α**), (**2β**), (**3**), and (**4**) (Figures 2—5) reveal some interesting features. Compounds (**2α**) and (**2β**) are polymorphs. The principal differences between the two forms are (*i*) in the orientation of the phosphine *trans* to N(1) relative to Br(1) (Figures 2 and 3) and (*ii*) in the hydrogen-bonding interactions. In (**2α**) the P(2) phosphine phenyl ring is *anti* to

Table 4. Atom co-ordinates ($\times 10^4$) for (2β)

Atom	*x*	*y*	*z*
Pt	3 051(1)	1 108(1)	3 046(1)
Br(1)	2 087(1)	538(1)	5 013(1)
Br(2)	4 403(1)	2 451(1)	3 973(1)
S(1)	5 841(2)	−574(2)	2 633(2)
S(2)	4 133(2)	1 450(2)	1 275(2)
P(1)	2 001(2)	−258(2)	2 163(2)
P(2)	1 484(2)	3 002(2)	2 711(2)
N(1)	4 630(5)	−396(5)	3 471(5)
N(2)	5 522(5)	386(6)	1 516(6)
C(1)	3 044(6)	−1 834(6)	2 321(6)
C(2)	3 938(7)	−2 192(7)	1 475(7)
C(3)	4 804(8)	−3 349(8)	1 651(8)
C(4)	4 792(9)	−4 144(8)	2 690(9)
C(5)	3 875(8)	−3 811(7)	3 521(8)
C(6)	3 011(7)	−2 653(7)	3 383(7)
C(7)	474(7)	−433(7)	2 785(8)
C(8)	1 689(7)	172(7)	572(6)
C(9)	−104(6)	2 870(6)	2 325(6)
C(10)	−525(7)	3 064(7)	1 132(7)
C(11)	−1 749(7)	3 026(7)	835(8)
C(12)	−2 582(7)	2 762(7)	1 750(8)
C(13)	−2 194(7)	2 562(8)	2 893(8)
C(14)	−949(7)	2 601(7)	3 206(7)
C(15)	1 259(7)	3 845(7)	4 020(7)
C(16)	1 996(7)	4 082(7)	1 558(7)
F(1)	1 650(5)	1 814(3)	8 158(6)
F(2)	−84(3)	3 363(7)	7 911(7)
F(3)	1 606(7)	3 642(6)	8 862(4)
F(4)	1 670(7)	3 547(6)	6 920(4)
F(5)	2 170(2)	2 392(3)	8 686(6)
F(6)	1 243(7)	4 339(3)	7 902(7)
F(7)	1 350(7)	2 716(8)	6 860(3)
F(8)	73(2)	2 918(7)	8 408(6)
B(1)	1 210(3)	3 091(3)	7 963(3)

Table 5. Atom co-ordinates ($\times 10^4$) for (3)

Atom	*x*	*y*	*z*
Pt	10 209(1)	3 874(1)	5 554(1)
Br	8 897(3)	2 616(1)	6 513(1)
S(1)	8 708(8)	3 692(3)	3 712(2)
S(2)	11 337(7)	4 925(2)	4 614(2)
P	11 900(6)	4 605(2)	6 604(2)
N(1)	8 570(23)	3 263(8)	4 606(6)
N(2)	10 195(28)	4 587(10)	3 741(8)
C(1)	13 432(22)	5 653(10)	6 320(7)
C(2)	12 668(31)	6 580(10)	6 446(8)
C(3)	13 853(38)	7 381(11)	6 195(9)
C(4)	15 778(33)	7 223(11)	5 836(9)
C(5)	16 539(37)	6 299(12)	5 630(11)
C(6)	15 376(21)	5 549(11)	5 901(12)
C(7)	13 795(30)	3 830(11)	7 140(9)
C(8)	9 999(38)	5 009(12)	7 402(8)

Br(1) [Br(1)–Pt–P(2)–C(9) torsion angle −176.0(5)°] whilst in (2β) the phenyl is approximately *gauche* with respect to Br(1) [Br(1)–Pt–P(2)–C(9) torsion angle −73.7(3)°].*

In both cases, the dominant feature in the packing of the ions is the hydrogen bond formed through N(1)–H. In (2α) the hydrogen bond is to a fluorine, F(1), of a neighbouring BF_4^- anion [N(1)···F(1) 2.93 Å]. In (2β) the hydrogen bond is to Br(2) of another cation [N(1)···Br(2) 3.44 Å] which is related by a crystallographic centre of symmetry (Figure 3). The cations in (2β) thus exist in the crystal as hydrogen-bonded dimers.

The only significant difference in the bonding within the cations of (2α) and (2β) is a slight shortening of the Pt–Br(2)

* ^{1}H N.m.r. solution studies on (2α) and (2β) reveal four methyl resonances (split into doublets by ^{31}P) between δ 1.8 and 2.3 with no noticeable variation in the spectra in the temperature range −70 to +70 °C.

Table 6. Atom co-ordinates ($\times 10^4$) for (4)

Atom	*x*	*y*	*z*
Pt	9 743(1)	8 905(1)	9 483(1)
I	11 130(2)	7 534(1)	8 512(1)
S(1)	11 311(11)	8 851(4)	11 308(3)
S(2)	8 671(10)	10 000(3)	10 389(3)
P	8 025(7)	9 569(3)	8 428(3)
N(1)	11 411(31)	8 388(10)	10 421(9)
N(2)	9 899(43)	9 734(13)	11 242(11)
C(1)	6 499(28)	10 608(12)	8 725(12)
C(2)	4 588(43)	10 455(15)	9 091(19)
C(3)	3 462(47)	11 240(19)	9 295(21)
C(4)	4 339(58)	12 191(16)	9 193(18)
C(5)	6 128(47)	12 314(19)	8 840(16)
C(6)	7 151(40)	11 532(12)	8 597(13)
C(7)	6 300(42)	8 765(15)	7 906(15)
C(8)	9 773(40)	9 968(14)	7 613(13)

Table 7. Selected bond lengths (Å) and angles (°) for (2α)

Pt–Br(1)	2.494(2)	Pt–Br(2)	2.549(2)
Pt–S(2)	2.329(4)	Pt–P(1)	2.346(3)
Pt–P(2)	2 318(3)	Pt–N(1)	2.109(8)
S(1)–N(1)	1.564(11)	S(1)–N(2)	1.541(12)
S(2)–N(2)	1 652(9)	P(1)–C(1)	1.815(11)
P(1)–C(7)	1.802(15)	P(1)–C(8)	1.800(14)
P(2)–C(9)	1.775(13)	P(2)–C(15)	1.807(13)
P(2)–C(16)	1.818(14)		
Br(1)–Pt–Br(2)	90.8(1)	Br(1)–Pt–S(2)	175.5(1)
Br(2)–Pt–S(2)	86.9(1)	Br(1)–Pt–P(1)	92.6(1)
Br(2)–Pt–P(1)	173.4(1)	S(2)–Pt–P(1)	89.3(1)
Br(1)–Pt–P(2)	88.4(1)	Br(2)–Pt–P(2)	89.2(1)
S(2)–Pt–P(2)	95.4(1)	P(1)–Pt–P(2)	96.5(1)
Br(1)–Pt–N(1)	90.6(3)	Br(2)–Pt–N(1)	83.4(3)
S(2)–Pt–N(1)	85.3(3)	P(1)–Pt–N(1)	90.9(3)
P(2)–Pt–N(1)	172.6(3)	N(1)–S(1)–N(2)	110.3(5)
Pt–S(2)–N(2)	101.9(4)	Pt–P(1)–C(1)	110.1(4)
Pt–P(1)–C(7)	116.0(5)	C(1)–P(1)–C(7)	105.2(6)
Pt–P(1)–C(8)	114.6(5)	C(1)–P(1)–C(8)	104.5(6)
C(7)–P(1)–C(8)	105.5(7)	Pt–P(2)–C(9)	112.0(4)
Pt–P(2)–C(15)	113.4(4)	C(9)–P(2)–C(15)	104.4(7)
Pt–P(2)–C(16)	115.4(5)	C(9)–P(2)–C(16)	108.1(6)
C(15)–P(2)–C(16)	102.5(7)	Pt–N(1)–S(1)	118.1(6)
S(1)–N(2)–S(2)	124.1(8)		

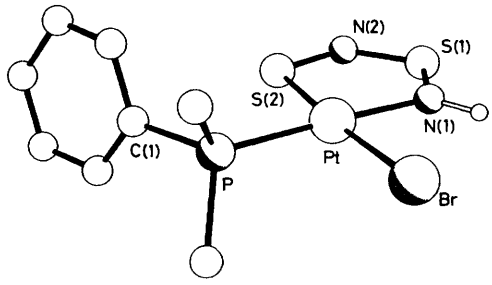

Figure 4. *X*-Ray crystal structure of [Pt(S_2N_2H)Br(PMe_2Ph)] (3)

Table 8. Selected bond lengths (Å) and angles (°) for (2β)

Pt–Br(1)	2.498(1)	Pt–Br(2)	2.562(1)
Pt–S(2)	2.324(2)	Pt–P(1)	2.345(2)
Pt–P(2)	2.335(2)	Pt–N(1)	2.083(5)
S(1)–N(1)	1.582(6)	S(1)–N(2)	1.522(6)
S(2)–N(2)	1.668(6)	P(1)–C(1)	1.807(6)
P(1)–C(7)	1.805(8)	P(1)–C(8)	1.810(7)
P(2)–C(9)	1.793(7)	P(2)–C(15)	1.807(8)
P(2)–C(16)	1.801(8)		
Br(1)–Pt–Br(2)	92.3(1)	Br(1)–Pt–S(2)	173.8(1)
Br(2)–Pt–S(2)	87.2(1)	Br(1)–Pt–P(1)	89.9(1)
Br(2)–Pt–P(1)	174.5(1)	S(2)–Pt–P(1)	90.0(1)
Br(1)–Pt–P(2)	90.8(1)	Br(2)–Pt–P(2)	85.9(1)
S(2)–Pt–P(2)	95.4(1)	P(1)–Pt–P(2)	99.2(1)
Br(1)–Pt–N(1)	89.6(2)	Br(2)–Pt–N(1)	84.5(2)
S(2)–Pt–N(1)	84.2(2)	P(1)–Pt–N(1)	90.4(2)
P(2)–Pt–N(1)	170.4(2)	N(1)–S(1)–N(2)	108.2(3)
Pt–S(2)–N(2)	102.3(2)	Pt–P(1)–C(1)	107.8(2)
Pt–P(1)–C(7)	116.5(3)	C(1)–P(1)–C(7)	106.9(3)
Pt–P(1)–C(8)	114.2(3)	C(1)–P(1)–C(8)	105.9(3)
C(7)–P(1)–C(8)	104.9(4)	Pt–P(2)–C(9)	117.3(2)
Pt–P(2)–C(15)	111.6(2)	C(9)–P(2)–C(15)	104.1(3)
Pt–P(2)–C(16)	109.9(2)	C(9)–P(2)–C(16)	107.9(3)
C(15)–P(2)–C(16)	105.3(4)	Pt–N(1)–S(1)	120.4(3)
S(1)–N(2)–S(2)	124.4(4)		

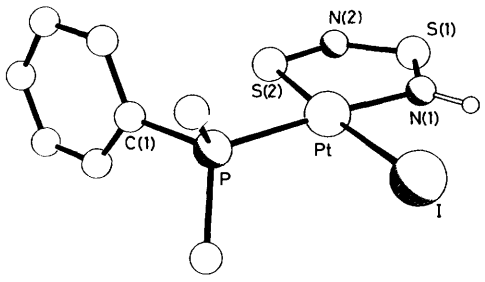

Figure 5. *X*-Ray crystal structure of $[Pt(S_2N_2H)I(PMe_2Ph)]$ (**4**)

bond in (**2α**) compared with its value in (**2β**) [2.549(2) *cf.* 2.562(1) Å]. This is probably due to a weakening in the Pt–Br(2) bond in (**2β**) associated with the formation of the N–H • • • Br hydrogen bond. The Pt–Br(1) bond lengths in both (**2α**) and (**2β**) [2.494(2), 2.498(1) Å] are shorter than Pt–Br(2) reflecting the difference in *trans* influence of phosphorus *versus* sulphur. Both structures show the slightly distorted octahedral environment at the platinum which is as expected. The Pt–S(2) bond lengths are in the order (**2α**) and (**2β**) > (**1a**) > (**3**) and (**4**) [2.329(4), 2.324(2) for (**2α**) and (**2β**); 2.283(2) for (**1a**);[4] and 2.222(3), 2.228(5) Å for (**3**) and (**4**)]. Thus there appear to be two different features affecting this bond length: (*i*) the oxidation state at platinum, Pt^{IV} resulting in longer Pt–S bonds than Pt^{II}; and (*ii*) the ligand *trans* to sulphur, halogens resulting in shorter Pt–S bonds than phosphines. The Pt–N and Pt–P bond lengths are shorter for all of the Pt^{II} complexes [(**1**), (**3**), and (**4**)] than for (**2α**) or (**2β**). The pattern of intermediate, short and long bonds in the sulphur–nitrogen portion of the metallacycle is similar to that observed in the previously reported Pt^{II} complexes of this ligand.[1,4]

Complexes (**3**) and (**4**) are isostructural. The only significant difference is the length of the crystallographic *a* axis (*ca.* 0.3 Å greater in the iodo complex). The substitution of I for Br does not greatly affect the geometry at the platinum, with only a slightly increased P–Pt–halogen angle [90.2(1) for (**3**), 91.0(1)° for (**4**)]. All of the other bond lengths and angles are not significantly altered. We have discussed the Pt–P, Pt–S, and Pt–N bond lengths relative to (**1**), (**2α**), and (**2β**) above. The pattern of bonding in the sulphur–nitrogen portion of the metallacycle is as observed previously in other Pt^{II} complexes.[1,4] It is interesting to note that the orientation of the phosphine in (**3**) and (**4**) mimics that in (**2α**) with the phenyl ring of the phosphine being *anti* to the halogen.

Table 9. Selected bond lengths (Å) and angles (°) for (**3**)

Pt–Br	2.475(1)	Pt–S(2)	2.222(3)
Pt–P	2.246(3)	Pt–N(1)	2.033(11)
S(1)–N(1)	1.564(10)	S(1)–N(2)	1.555(15)
S(2)–N(2)	1.652(14)	P–C(1)	1.803(14)
P–C(7)	1.825(17)	P–C(8)	1.848(19)
Br–Pt–S(2)	175.6(1)	Br–Pt–P	90.2(1)
S(2)–Pt–P	94.0(1)	Br–Pt–N(1)	90.5(3)
S(2)–Pt–N(1)	85.4(3)	P–Pt–N(1)	177.2(4)
N(1)–S(1)–N(2)	108.0(7)	Pt–S(2)–N(2)	105.0(5)
Pt–P–C(1)	115.1(4)	Pt–P–C(7)	113.8(5)
C(1)–P–C(7)	104.1(7)	Pt–P–C(8)	110.9(7)
C(1)–P–C(8)	106.3(7)	C(7)–P–C(8)	105.7(8)
Pt–N(1)–S(1)	120.6(7)	S(1)–N(2)–S(2)	120.9(8)

Table 10. Selected bond lengths (Å) and angles (°) for (**4**)

Pt–I	2.635(1)	Pt–S(2)	2.228(5)
Pt–P	2.250(5)	Pt–N(1)	2.010(17)
S(1)–N(1)	1.576(16)	S(1)–N(2)	1.545(23)
S(2)–N(2)	1.645(21)	P–C(1)	1.826(18)
P–C(7)	1.806(25)	P–C(8)	1.840(24)
I–Pt–S(2)	175.4(1)	I–Pt–P	91.0(1)
S(2)–Pt–P	93.4(2)	I–Pt–N(1)	90.1(4)
S(2)–Pt–N(1)	85.5(5)	P–Pt–N(1)	176.1(5)
N(1)–S(1)–N(2)	106.6(10)	Pt–S(2)–N(2)	104.1(8)
Pt–P–C(1)	113.7(6)	Pt–P–C(7)	115.0(7)
C(1)–P–C(7)	105.2(10)	Pt–P–C(8)	110.5(8)
C(1)–P–C(8)	107.4(9)	C(7)–P–C(8)	104.3(11)
Pt–N(1)–S(1)	121.3(10)	S(1)–N(2)–S(2)	122.3(11)

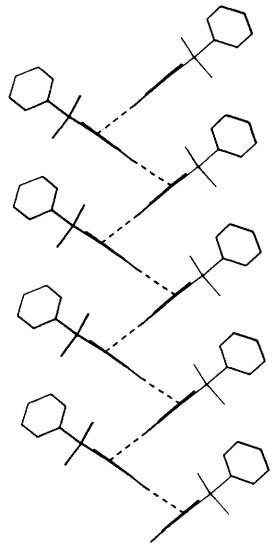

Figure 6. View showing the herring-bone packing in (**3**)

A significant feature of both (**3**) and (**4**) is the herring-bone packing array (Figure 6) of the molecules and the associated N–H • • • Pt contacts, with the N–H bond directed toward the Pt d_{z^2} orbital of another molecule related by a 2_1 screw axis in the crystallographic *a* direction. These contacts are for (**3**) H • • • Pt 2.73 Å and for (**4**) H • • • Pt 2.94 Å.

Acknowledgements

We are grateful to Johnson Matthey plc for loans of precious metals and to the University of London Central Research fund for an equipment grant.

References

1 R. Jones, C. P. Warrens, D. J. Williams, and J. D. Woollins, *J. Chem. Soc., Dalton Trans.*, 1987, 907.
2 R. Jones, P. F. Kelly, D. J. Williams, and J. D. Woollins, *Polyhedron*, 1987, **6**, 1541.
3 R. Jones, P. F. Kelly, C. P. Warrens, D. J. Williams, and J. D. Woollins, *J. Chem. Soc., Chem. Commun.*, 1986, 711.
4 R. Jones, P. F. Kelly, D. J. Williams, and J. D. Woollins, *J. Chem. Soc., Dalton Trans.*, 1988, 803.
5 G. M. Sheldrick, SHELXTL, An Integrated system for solving, refining, and displaying crystal structures from diffraction data, University of Göttingen, Federal Republic of Germany, 1978; Revision 4.1, 1983.
6 'International Tables for *X*-Ray Crystallography,' Kynoch Press, Birmingham, 1974, vol. 4, pp. 99—149.

Received 8*th July* 1987; *Paper* 7/1224